Behavioral/Cognitive

Whole-Brain Deactivations Precede Uninduced Mind-Blanking Reports

Paradeisios Alexandros Boulakis,[1,2] Sepehr Mortaheb,[1,2] Laurens van Calster,[2,3,4,5] Steve Majerus,[2,3,4] and Athena Demertzi[1,2,3]

[1]Physiology of Cognition Lab, GIGA-Cyclotron Research Center In Vivo Imaging, University of Liège, Liège 4000, Belgium, [2]National Fund for Scientific Research (FNRS), Brussels 1000, Belgium, [3]Psychology and Neuroscience of Cognition Research Unit, University of Liège, Liège 4000, Belgium, [4]GIGA-Cyclotron Research Center In Vivo Imaging, University of Liège, Liège 4000, Belgium, and [5]Department of Neurology, Cliniques Universitaires Saint-Luc, Brussels 1200, Belgium

Mind-blanking (MB) is termed as the inability to report our immediate-past mental content. In contrast to mental states with reportable content, such as mind-wandering or sensory perceptions, the neural correlates of MB started getting elucidated only recently. A notable particularity that pertains to MB studies is the way MB is instructed for reporting, like by deliberately asking participants to "empty their minds." Such instructions were shown to induce fMRI activations in frontal brain regions, typically associated with metacognition and self-evaluative processes, suggesting that MB may be a result of intentional mental content suppression. Here, we aim at examining this hypothesis by determining the neural correlates of MB without induction. Using fMRI combined with experience-sampling in 31 participants (22 female), univariate analysis of MB reports revealed deactivations in occipital, frontal, parietal, and thalamic areas, but no activations in prefrontal regions. These findings were confirmed using Bayesian region-of-interest analysis on areas previously shown to be implicated in induced MB, where we report evidence for frontal deactivations during MB reports compared with other mental states. Contrast analysis between reports of MB and content-oriented mental states also revealed deactivations in the left angular gyrus. We propose that these effects characterize a neuronal profile of MB, where key thalamocortical nodes are unable to communicate and formulate reportable content. Collectively, we show that study instructions for MB lead to differential neural activation. These results provide mechanistic insights linked to the phenomenology of MB and point to the possibility of MB being expressed in different forms.

Key words: **angular gyrus; anterior cingulate cortex; fMRI; experience-sampling; mental content; mind-blanking; spontaneous thinking**

Significance Statement

This study explores how brain activity changes when individuals report unidentifiable thoughts, a phenomenon known as mind-blanking (MB). It aims to detect changes in brain activations and deactivations when MB is reported spontaneously, as opposed to the neural responses that have been previously reported when MB is induced. By means of brain imaging and experience-sampling, the study points to reduced brain activity in a wide number of regions, including those mesio-frontally which were previously detected as activated during induced MB. These results enhance our understanding of the complexity of spontaneous thinking and contribute to broader discussions on consciousness and reportable experience.

Introduction

During spontaneous thinking mental content appears continuous and seamless (Christoff et al., 2009). Probing people to report what they think yields various mental states with distinct contents and attitudes toward those contents, such as daydreaming, task engagement, and mind wandering (Van Calster et al., 2017; Smallwood et al., 2021). A critical component of these states is the presence of content. Recently, however, the study of unconstrained cognition has begun to focus on the experience of the inability to report on immediate mental content, termed mind-blanking (MB; Ward and Wegner, 2013).

Received Apr. 10, 2023; revised July 11, 2023; accepted Aug. 7, 2023.

Author contributions: P.A.B. and A.D. designed research; L.v.C. performed research; P.A.B. and S.Mo. analyzed data; P.A.B. and A.D. wrote the first draft of the paper; S.Mo., L.v.C., and S.Ma. edited the paper; P.A.B. and A.D. wrote the paper.

This work was supported by the Belgian Fund for Scientific Research (FRS-FNRS), the European Union's Horizon 2020 Research and Innovation Marie Skłodowska-Curie RISE programme *NeuronsXnets* (grant agreement 101007926), the European Cooperation in Science and Technology COST Action (CA18106), the Léon Fredericq Foundation, and the University and of University Hospital of Liège.

The authors declare no competing financial interests.

Correspondence should be addressed to Athena Demertzi at a.demertzi@uliege.be.

https://doi.org/10.1523/JNEUROSCI.0696-23.2023

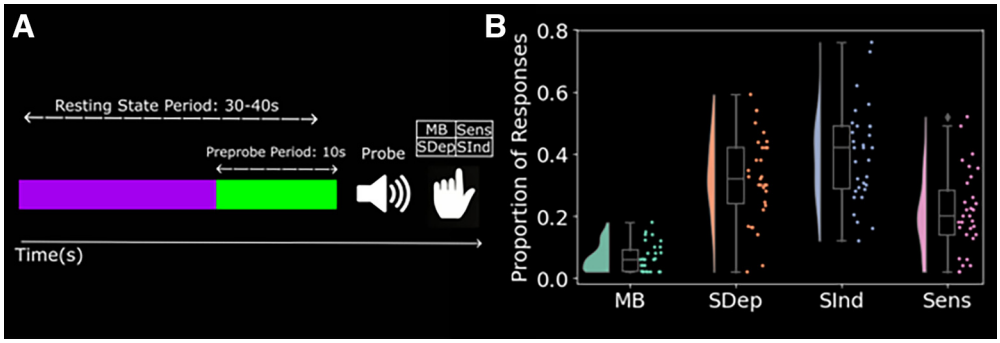

Figure 1. The experience-sampling paradigm. ***A***, Single trial example. During experience-sampling participants are asked to restfully lay in the scanner with eyes open and let their mind wander without any further orientation as to the focus of their thoughts. At random intervals (30–60 s), participants are probed with an auditory cue to report the content of their thoughts at the moment preceding the probe using button press. Four available report categories were presented as available: mind-blanking (MB), perceptions (Sens), stimulus-independent thoughts (SInd), and stimulus-dependent thoughts (SDep). For subsequent analysis, only the final 10 s of the resting period (green segment) were used. ***B***, Raincloud plots showing MB was reported at lower rates compared with mental states with content. Density kernels show how data are distributed and where peaks where aggregated. Boxplots show interquartiles ranges and medians. Pointplots show individual datapoints.

Recent research into the neural correlates of MB using fMRI experience-sampling (i.e., asking people at random times to report their immediate mental state; Smallwood and Schooler, 2015; Weinstein, 2018) showed that spontaneous MB reports were close to a cerebral configuration characterized by a positive all-to-all connectivity profile (Mortaheb et al., 2022). Such a pattern of overall positive statistical dependencies implies that all cortical regions communicate in the same way when MB is reported. It is of interest that similar functional organization is observed in NREM sleep (El-Baba et al., 2019), suggesting that MB might be the result of overall low cortical arousal. Similar evidence was found on shorter timescales using EEG, where localized slow-wave activity was linked with MB reports, leading to the possibility of cerebral "local sleeps" during MB (Andrillon et al., 2019). Indeed, posterior electrode slow-wave activity during a go/no-go task was predictive of MB reports, in contrast to frontal electrode slow-waves, which were linked to mind-wandering (Andrillon et al., 2021). Collectively, these studies propose that MB events are tied to neuronal profiles which do not permit efficient cortical communication, therefore hindering people from reporting clear mental content (Mortaheb et al., 2022).

A notable particularity of MB studies is the way MB is instructed for report. For example, Kawagoe et al. (2019) studied MB by asking people to actively "empty their minds" until they experience no thoughts, upon when they reported they had achieved this state. By analyzing the fMRI BOLD signal preceding these reports, the authors found deactivations in Broca's area and the left hippocampus, and activations in the ventromedial prefrontal cortex (vmPFC)/subgenual region of the anterior cingulate cortex (subACC). The authors interpreted these results as reduced inner speech, elicited by the attempt of participants to silence internally generated thoughts. This possibility was considered by other authors, too, primarily in the context of mind wandering: As our thoughts spontaneously transition across an internal-external milieu (Vanhaudenhuyse et al., 2011; Smallwood et al., 2012; Demertzi et al., 2013), the ACC serves executive functions, such as identifying attentional lapses from ongoing tasks (Christoff et al., 2009) or allowing thought transitions to be controlled (Crespo-García et al., 2022). In similar lines, self-induced MB also requires constant supervision of thoughts in the form of evaluating ongoing experience to promote thought-silencing, therefore recruiting regions such as the vmPFC/subACC, a central hub for mental state evaluative processes (Jenkins and Mitchell, 2011; Qin et al., 2020). However, a hyperexperienced meditator showed decreases in fMRI connectivity between the posterior cingulate cortex and mesio-frontal regions when he was practicing content-free versus content-related meditation (Winter et al., 2020). Taken together, the use of MB induction in neuroimaging studies might provide a biased picture about the underlying neural mechanisms of MB that incorporates task demands of thought monitoring.

In the present work, we test the hypothesis that uninduced MB reports are linked to frontal deactivations, inverting the pattern observed in self-induced MB. By means of fMRI and experience-sampling, we first performed a univariate analysis to test whether MB reports would indicate frontal deactivations in the periods preceding MB reports, while remaining agnostic as to the contribution of the remaining cortex. To supplement our hypothesis of frontal deactivations, we performed ROI analysis to examine the specificity of deactivations in the vmPFC-subACC and other previously identified MB-related clusters.

Materials and Methods

Experience-sampling dataset/experimental design

We used previously collected data (Van Calster et al., 2017) acquired during resting-state with eyes open in a 3T head-only scanner (Magnetom Allegra, Siemens Medical Solutions). At random intervals ranging from 30 to 60 s, participants were probed with an auditory cue to report via button press what was in their mind at the moment just preceding the cue. Each probe started with the appearance of an exclamation mark lasting for 1000 ms inviting the participants to review and characterize the cognitive event(s) they just experienced. After this period, participants were presented with four options, classifying their mental content as: (1) absence, defined as MB or empty state of mind; (2) perceptions, defined as thought-free attentiveness to stimuli via the senses; and (3) thoughts (Fig. 1*A*). In the case of a "thought" report, participants were asked to report if the content was stimulus-dependent (SDep; thoughts evoked from the immediate environment) or stimulus-independent (SInd; thoughts irrelevant from the immediate environment). Depending on the probes' trigger times and participants' reaction times, the duration of the recording session was variable (48–58 min). To minimize misclassification rates, participants had a training session outside of the scanner at least 24 h before the actual session.

The dataset contains structural and functional MRI volumes for 36 healthy, right-handed participants (27 female, mean = 23, SD = 3, range = [18,30]). Five participants were excluded as they did not report

each mental state option at least once (total participants = 31, 22 female). Overall, participants reported MB 6% of total reports (SD: 0.04, range: [1,9]) Sens 20% of trials (SD: 0.13, range: [1,26]) SDep 32% of total reports (SD: 0.14, range: [1,29]), and SInd 42% of total reports (SD: 0.15, range: [6,28]) (Fig. 1*B*). All participants gave their written informed consent to take part in the experiment. The study was approved by the ethics committee of the University Hospital of Liège.

FMRI acquisition parameters

FMRI data were acquired with standard transmit–receive quadrature head coil using a T2*-weighted gradient-echo EPI sequence with the following parameters: repetition time (TR) = 2040 ms, echo time (TE) = 30 ms, field of view (FOV) = 192 × 192 mm2, 64 × 64 matrix, 34 axial slices with 3-mm thickness and 25% interslice gap to cover most of the brain. A high-resolution T1-weighted MP-RAGE image was acquired for anatomic reference (TR = 1960 ms, TE = 4.4 ms, inversion time = 1100 ms, FOV = 230 × 173 mm, matrix size = 256 × 192 × 176, voxel size = 0.9 × 0.9 × 0.9 mm). The participant's head was restrained using a vacuum cushion to minimize head movement. Stimuli were displayed on a screen positioned at the rear of the scanner, which the participant could comfortably see using a head coil-mounted mirror.

Statistical analysis

Preprocessing

Structural and functional images were preprocessed using a locally developed pipeline written in the Nipype module (v1.8.2; https://nipype.readthedocs.io/) in Python (v3.8), combining functions from Statistical Parametric Mapping software (SPM12; https://www.fil.ion.ucl.ac.uk/spm/), the FMRIB Software Library v6.0 (FSL; https://fsl.fmrib.ox.ac.uk/fsl/fslwiki), and the Artifact Detections Tools (ART; https://www.nitrc.org/projects/artifact_detect). For each node of the pipeline, we have specified the respective module and function used. Structural images were skull stripped (fsl.Bet), bias-field corrected, and segmented into white matter, gray matter, and cerebrospinal fluid (spm.Segment). Finally, the restored, bias-corrected structural image was normalized into the standard stereotaxic Montreal Neurologic Institute (MNI) space (spm.Normalize). The first four volumes (8.16 s) of the functional data were removed to avoid T1 saturation effects (fsl.ExtractROI). The volumes were slice-scan time corrected to account for the accumulation of offset delays between the first slice and the remaining slices (fsl.SliceTimer). Then, the scans were realigned to the mean functional volume (spm.Realign) using a second B-spline interpolation with least-squares alignment. We used the realignment parameters to estimate motion outlier scans. An image was defined as an outlier or artifact image if the head displacement in the *x*, *y*, or *z* direction was >3 mm from the previous frame, if the rotational displacement was >0.05 rad from the previous frame, or if the global mean intensity in the image was >3 SDs from the mean image intensity for the entire scans. The realignment parameters were also saved so that these variables can be used as regressors when modeling subject-level BOLD activity. Then, the images were coregistered to the participant space using the bias-corrected structural image as the target and a normalized mutual information function (spm.Coregister) and then normalized to MNI space (spm.Normalize). Finally, the normalized images were smoothed using a Gaussian kernel of 8 mm full width at half-maximum. For comparability purposes, the preprocessing pipeline followed the approach as in previous works with this dataset (Van Calster et al., 2017) with MB analysis (Kawagoe et al., 2019).

Univariate whole-brain analysis

Data were analyzed using a univariate linear general linear model (GLM). The four responses of the participants (MB, SDep, SInd, Sens) were modeled and convolved with the canonical hemodynamic response function (HRF) as regressors of interest for each participant in the first-level analysis. Each response instance was modeled as an epoch starting five TRs before probe onset, following evidence from a "thinking aloud" paradigm that showed that mental states tend to fluctuate slowly, with one experience being reported every 10 s (Van Calster et al., 2017). Each participant's six motion parameters (three rigid body translations and three rotations from the realignment procedure) were included to regress out effects related to head movement-related variability. We used a high-pass filter cutoff of 1/128 Hz to remove the slow signal drifts with a longer period, and a first-order autoregressive model [AR (1)] was used for serial correlations with the classical restricted maximum likelihood (REML) parameter. Regionally specific condition effects were tested using linear contrasts for each key event relative to the baseline and each participant. Contrasts for "Perception" and "Thinking" regressors have been reported elsewhere (Van Calster et al., 2017). Therefore, we tested for contrasts specific to MB. Given four regressors: [MB, Sens, SDep, SInd], subject-level analysis yielded the following T contrasts of interest: (1) positive effects of MB [1 0 0 0], (2) negative effects of MB [−1 0 0 0], (3) MB > Thinking [2 0 −1 −1], (4) Thinking > MB [−2 0 1 1], (5) MB > Sens [1 −1 0 0], (6) Sens > MB [−1 1 0 0], (7) Absence > Content [3 −1 −1 −1], (8) Content > Absence [−3 1 1 1]. The resulting contrast parameter estimates from the individual subject-level were entered into a random effects model for a second level analysis, using a one-sided, one-sample *t* test. Regarding result reporting and visualization, we have opted for a "don't hide/highlight" approach (Taylor et al., 2023), effectively presenting all relevant maps at $p_{uncorrected} < .001$ and by annotating the contours of statistically significant clusters at $p\text{FDR} < 0.05$. Exploratory analysis will be conducted at clusters with voxel size >50. Interactive 3D surface projections of the contrasts presented in results are available on https://gitlab.uliege.be/Paradeisios.Boulakis/mb_activation/-/tree/main/plotting. The unthresholded maps are publicaly available at Neurovault: https://identifiers.org/neurovault.collection:14761.

Region-of-interest (ROI) analysis

Based on the a-priori hypothesis about the role of the ACC in monitoring thought contents, we additionally performed a ROI analysis based on MNI coordinates reported in Kawagoe et al. (2019) for the ACC (MNI: 3,39,−5). To examine whether previous findings on the neuronal correlates of MB during active mental silencing can be extended to spontaneous blanking periods in ongoing mentation, we also included the left hippocampus (MNI: −27,−33,−3) and Broca's area (MNI: −47,26,20). To extract single-participant β parameters for each regressor of interest, 5-mm radius binary spheres were created for each ROI using the flsmaths function of the FSL software, which were then used to mask first-level subject-specific β parameter maps, and extract the signal of interest. Localization of the ROIs was performed based on the MNI coordinates reported in Kawagoe et al. (2019).

Given our hypothesis for the absence of frontal engagement in MB and the reduced statistical power of traditional frequentist approaches because of multiple comparisons, we opted for Bayesian linear modeling (McElreath, 2020), allowing us to make inferences on potential null results while not being overly conservative. For each ROI, we fit a linear model with β values as a dependent variable, allowing the intercept to freely vary as a function of mental state:

$$Beta \sim a[mental\,state] + error.$$

As prior for the intercept we chose a normal distribution as it is the maximum entropy distribution (or "least surprising") for any random variable with an unknown mean and unknown, finite variance. Effectively, a maximum entropy distribution is the most probable distribution for a random variable, given the potential constraints placed on its parameters. We chose to model the intercepts as $N(0, 1)$, as we expected small effects. To examine the robustness of our choice of priors, we constructed two variants of normal distributions, one skeptical distribution that reduces effect sizes close to 0 by having high precision, marked as low variance $N(0, .5)$, and one lax prior, marked by low precision, permitting extreme effects $N(0, 3)$. Prior predicative simulation for the skeptical prior places the mass of effect sizes of each state within half a standard deviation from the mean. Likewise, the lax prior places the mass of effect sizes within three standard deviations. Additionally, we also fit a model using a uniform prior $U(-2, 2)$, giving equal probability to effect sizes within two standard deviations from the mean. To further validate that our priors

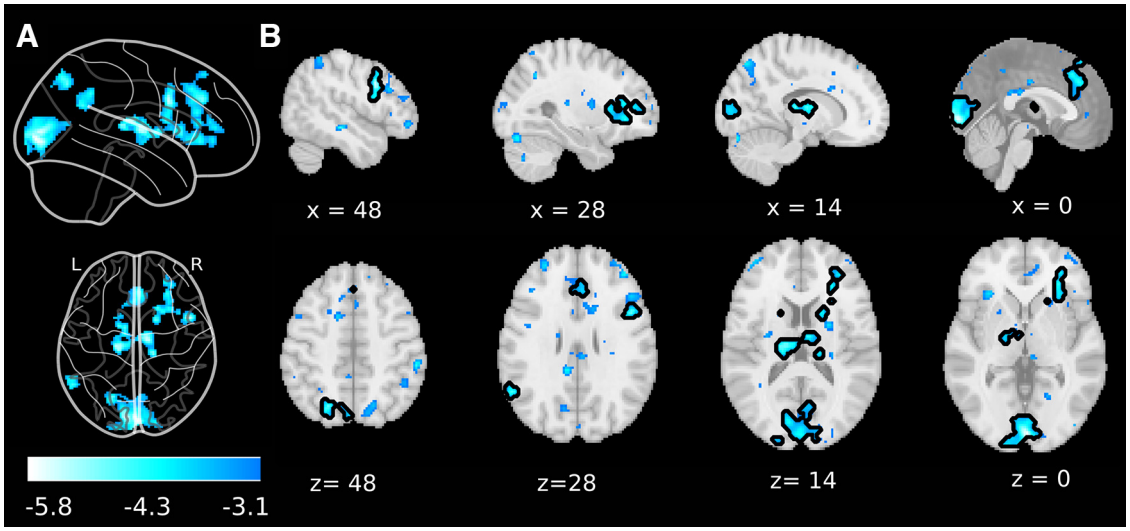

Figure 2. FMRI univariate analysis of MB reports reveals whole-brain deactivations. Statistically significant deactivations were observed in the anterior cingulate cortex, the calcarine cortex, the bilateral thalami, the right anterior insula, the precentral gyrus, the left superior parietal lobule, the inferior frontal gyrus and the right operculum. ***A***, Glass brain projection (sagittal and axial views) at voxel-level $p_{uncorrected} < 001$, and cluster level $p_{FDR} < .05$. Color-bar indicates *t* statistic. ***B***, Activation maps of negative MB effects projected on the MNI152 cortical template (sagittal and axial views). Maps are calculated on 10 s preceding MB reports. The deactivated map projection is performed at voxel-level $p_{uncorrected} < .001$. Black contours signify the clusters that were significance at $p_{FDR} < .05$.

generated the desired ranges of parameters, we sampled from the prior distribution to perform a prior predictive visual check.

We estimated one posterior distribution for each one of the intercepts of the four mental states. Difference posterior was estimated by the pairwise subtraction of the mental state intercepts. Posterior distributions are summarized by their median, their standard deviation, and the 95% highest density intervals (HDIs), representing the 95% probability that the true parameter lies within that range. To validate that the posterior accurately represented a generative model of the data, we also performed posterior predictive simulations, to examine whether the ranges of our model can encompass the different β values.

To fit the models, we used a Markov Chain Monte-Carlo No U-Turn Sampler (MCMC-NUTS). MCMC is a class of algorithms for sampling from an unknown posterior distribution. The sampler uses a stochastic, random-walk procedure to draw samples from a random variable, and then approximates the desired distribution by integrating across the sum of the drawn samples (Harrison, 2010). The NUTS sampler is the mechanism of effective sample generation. As MCMC is sensitive to its tuning parameters, NUTS facilitates the sampling process by providing good candidate points in the distribution for the algorithm to sample (Hoffman and Gelman, 2014). To examine the convergence of the models, we sampled the posterior from four different chains, and both visually inspected the traceplot for points in the sampling procedure where the sampler stuck and accepted a model only if its scale reduction factor was at 1.00 (Fig. 4*B*). The stability of estimates was evaluated using an effect sample size (ESS) > 10,000. We sampled 5000 samples from the posterior, with 2000 samples as burn-in.

Each model was compared with a null model:

$$Beta \sim a + error,$$

where the intercept does not differentiate between the mental states, effectively representing the mean of the mental states. Model fitting was performed using the PYMC3 (https://docs.pymc.io/en/v3/index.html) Python package Salvatier et al. (2016).

Code accessibility

All codes to replicate the analysis is available on https://gitlab.uliege.be/Paradeisios.Boulakis/mb_activation (Boulakis, 2023). The code is based on existing Python libraries and custom functions. The provided repository contains all the necessary information to install an environment and reproduce the analysis on the experience-sampling dataset. We used an existing experience-sampling dataset, during which participants had the option to report the absence of thoughts (Van Calster et al., 2017). Previous research on this dataset, examining has replicated consistent fMRI findings in other mental states (MW: DMN and executive cortical areas). The raw data are also freely available in BIDS format from: https://openneuro.org/datasets/ds004134/versions/1.0.0. The unthresholded maps present in this paper can be found at https://identifiers.org/neurovault.collection:14761.

Table 1. FMRI Univariate analysis reveals deactivations during five TRs preceding MB reports

Region	No. of voxels	Z peak	*x*	*y*	*z*
Right calcarine cortex	1491	4.68	2	−92	0
Left calcarine cortex		4.54	−8	−88	6
Inferior frontal gyrus	243	4.51	48	10	32
Right operculum		3.76	48	10	22
Right thalamus	617	4.49	12	−12	8
Left thalamus		4.49	−18	−18	16
Superior frontomedial gyrus	472	4.21	2	36	34
Right anterior cingulate cortex		4.00	5	34	22
Left anterior cingulate cortex		3.55	−1	31	21
Left superior parietal lobule	187	4.14	−22	−68	46
Left precuneus		3.56	−4	−76	50
Right anterior insula	510	4.09	30	17	8
Right caudate		4.09	18	8	16
Left supramarginal gyrus	164	3.99	−58	−56	28

An uncorrected voxel-level threshold of $p = 0.01$ was set and FDR-corrected at the cluster level $p < 0.05$. The *x*-, *y*-, and *z*-coordinates refer to the AAL anatomic labeling map.

Results

fMRI univariate analysis reveals whole-brain deactivations

Initially, we focused on identifying regions associated with spontaneous MB occurrence during ongoing mentation. Overall, we found deactivations in the anterior cingulate cortex, the calcarine cortex, the bilateral thalami, the right anterior insula, the precentral gyrus, the left superior parietal lobule, the inferior frontal gyrus and the right operculum (Fig. 2; Table 1). To validate these results, we examined different TRs around the probe period. Although an uncorrected voxel-level threshold of $p = 0.01$

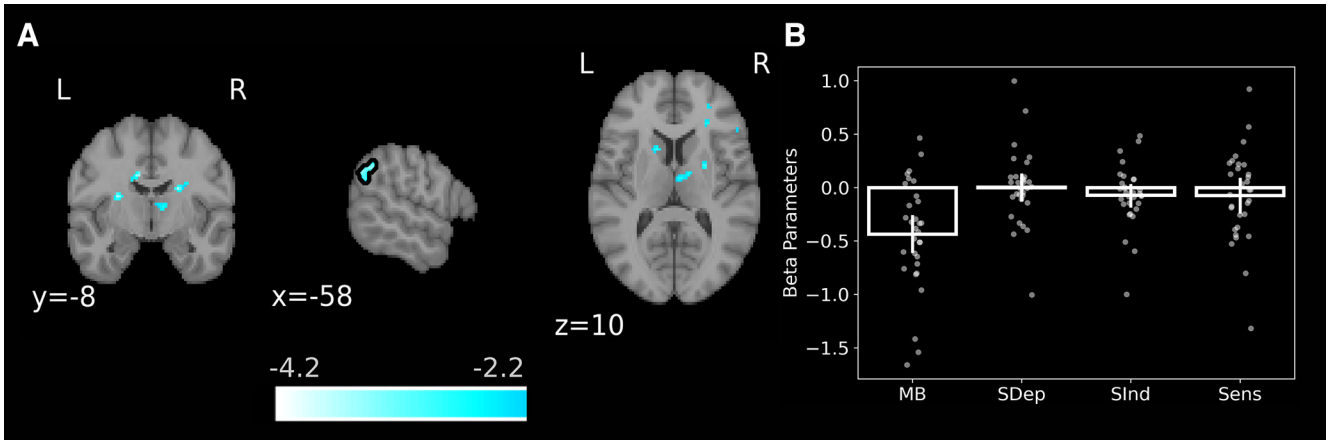

Figure 3. FMRI contrast analysis between content-oriented reports and MB at a lower exploratory threshold reveals deactivations in the left angular gyrus. ***A***, Activation map of presence versus absence of content contrast, projected on the MNI152 cortical template. The deactivated map projection is performed at voxel-level $p_{uncorrected} < 001$. Black contours signify the clusters that were significance at a cluster-extent threshold >50 voxels. Color-bar indicates *t* statistic. ***B***, Boxplots representing the β parameters of each mental state in left angular gyrus cluster. Error bars indicate 95% confidence intervals. Datapoints show single-subject parameter values. MB: mind-blanking, SDep: stimulus-dependent thoughts, SInd: stimulus-independent thoughts, Sens: perceptions.

recurrently showed deactivations in frontal, parietal and thalamical regions, cluster correction showed that only the thalamus was consistently deactivated across all time increments. Additionally, to control potential movement effects specific to conditions we estimated the overall framewise displacement of each subject at each time point (Power et al., 2012). Participants did not move significantly when considering displacement values per mental state category (mean: M; standard deviation: SD, confidence interval: CI) (MB: M = −0.006, SD = 0.182, CI = [−0.022, 0.009], SInd: M = −0.003, SD = 0.143, CI = [−0.008, 0.002], SDep: M = −0.004, SD = 0.161, CI = [−0.01, 0.003], Sens: M = −0.006, SD = 0.254, CI = [−0.018, 0.007]). Also, no significant difference was observed in terms of displacement values across mental states ($F_{(1,4)} = 0.146$).

At the FDR cluster threshold ($p<0.05$), the contrast between MB and the other mental states did not identify significant number of voxels. When the threshold was lowered to the exploratory level of whole-brain $p<0.001$, voxels >50, deactivations were observed in the angular gyrus (*n* voxels: 64, Z = 3.68, $x = -60$, $y = -58$, $z = 32$), a finding mainly driven by consistent deactivation of MB reports compared with stimulus dependent and stimulus independent thoughts (Fig. 3). An examination of the individual regressor sign of activation (positive/negative) shows that MB tended to be significantly deactivated. On the other side, the other three mental states varied around 0, and as their confidence intervals included 0, we cannot clearly estimate the direction of their activation.

Table 2. Descriptive statistics for the posterior distributions of the β parameters for each ROI and mental state

Region of interest	Contrast	Median	SD	HDI (0.025)	HDI (0.975)
vmPFC-ACC	MB	−0.242	0.119	−0.471	−0.01
	SDep	0.072	0.118	−0.158	0.306
	SInd	0.123	0.118	−0.114	0.35
	Sens	−0.027	0.119	−0.262	0.204
	MB-All	−0.298	0.119	−0.527	−0.064
	MB-SDep	−0.314	0.167	−0.64	0.013
	MB-SInd	−0.366	0.167	−0.693	−0.04
	MB-Sens	−0.214	0.168	−0.547	0.111
Broca's area	MB	−0.245	0.091	−0.429	−0.072
	SDep	−0.064	0.091	−0.242	0.112
	SInd	−0.205	0.09	−0.384	−0.031
	Sens	−0.202	0.091	−0.378	−0.021
	MB-All	−0.088	0.091	−0.272	0.085
	MB-SDep	−0.18	0.129	−0.434	0.069
	MB-SInd	−0.041	0.129	−0.287	0.216
	MB-Sens	−0.043	0.128	−0.289	0.21
Left hippocampus	MB	−0.113	0.056	−0.219	−0.001
	SDep	−0.119	0.056	−0.229	−0.009
	SInd	−0.069	0.055	−0.178	0.041
	Sens	−0.177	0.056	−0.287	−0.068
	MB-All	0.009	0.056	−0.098	0.121
	MB-SDep	0.007	0.079	−0.15	0.162
	MB-SInd	−0.044	0.079	−0.198	0.111
	MB-Sens	0.064	0.079	−0.094	0.217

HDI = highest density interval.

fMRI bayesian ROI analysis provides evidence of deactivations in the vmPFC/subACC

Based on our a-priori assumptions about the role of vmPFC/subACC in thought monitoring, we examined the activation effects in the clusters reported in Kawagoe et al. (2019), namely, the vmPFC/subACC, Broca's area and the left hippocampus. Extensive descriptive statistics of the posterior distributions for each ROI and mental state are presented in Table 2. Overall, the three ROIs' MB intercepts did not include 0 in their 95% credibility intervals (vmPFC/subACC = median: −0.242, SD: 0.119, HDI: [−0.471, −0.01], Broca's area = median: −0.245, SD: 0.091, HDI: [−0.429, −0.07], left hippocampus = median: −0.113, SD: 0.056, HDI: [−0.219, −0.001]; Fig. 4*C*), suggestive of functional deactivations in these clusters. To examine whether the clusters showed specificity in MB compared with the other mental states, pairwise comparisons between the MB β parameters and the betas of each other mental state were calculated, as well as an overall MB versus rest contrast. Pairwise comparison inference was performed by subtracting the MB posterior of each ROI from the posterior of the other mental states (Table 2). We found evidence only for the vmPFC/subACC cluster, namely MB reports were associated with reliably lower β values compared with the other mental states (median = −0.298, SD: 0.119, HDI: [−0.527, −0.054]). Additionally, we found significant effects for the contrast MB-SInd (median = −0.366, SD: 0.167, HDI: [−0.693, −0.064]; Fig. 4*E*,*G*,*I*). Compared with the other mental states, MB was the only report category that was

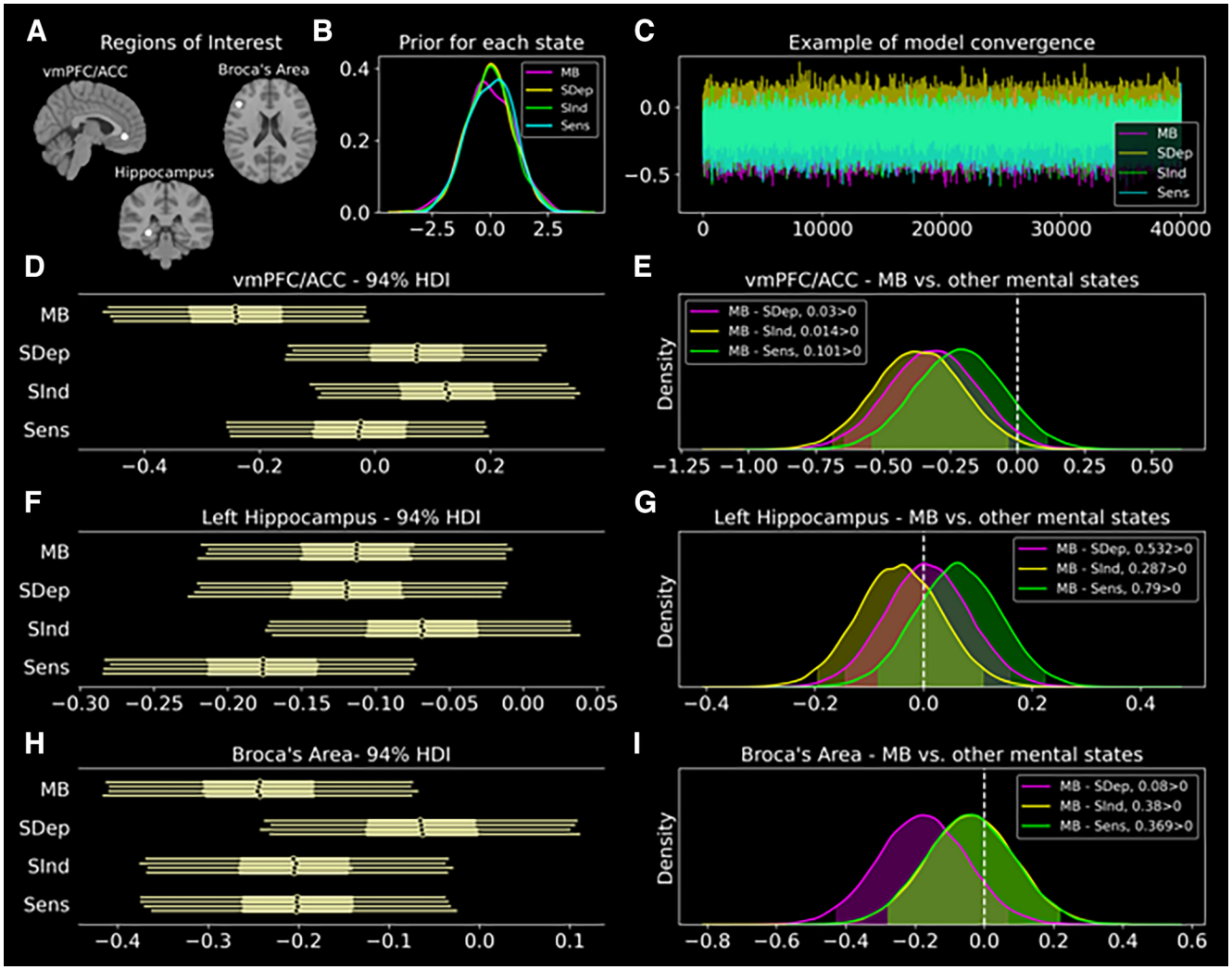

Figure 4. Bayesian analysis of the β parameters in the vmPFC/ACC ROI reveals MB-related deactivations in this cluster. ***A***, Regions of interest based on coordinates reported in Kawagoe et al. (2019) in the vmPFC/ACC, Broca's area, and the left hippocampus. ***B***, Null model prior expectations, modeling each prior as $N(0, 1)$. ***C***, Example traceplot of the model fit. Visual inspection of the random walk indicates that models converged, as the chains sampled the whole posterior space without autocorrelated data and sequential sampling of the same posterior space. ***D***, Forest plot of each of the four sampled chains of the posterior distribution indicate that vmPFC/ACC contains significant evidence for MB deactivations, as the β values did not contain 0 in the 94% highest density interval (HDI). Each line represents 94% highest HDIs. This was not the case for the rest of the mental states. ***E***, Posterior differences between MB and the other mental states. We observed that the contrast MB-SInd did not contain 0 in the 94% HDI (shaded area), providing evidence that frontal deactivations differentiated between MB and SInd. ***F***, Forest plot of each of the four sampled chains of the posterior distribution indicate that the left hippocampus is deactivated only in MB. This was also the case for SDep and Sens. ***G***, Posterior differences between MB and the rest of the mental states at the left hippocampus. We observed that no contrast indicated any specificity of the ROI in MB. ***H***, Forest plot of each of the four sampled chains of the posterior distribution indicate that the Broca's area contains evidence for MB contributions, as it does not contain 0 in the HDI. This was also the case for SInd and Sens. ***I***, Posterior differences between MB and the rest of the mental states the Broca's area. We observed that no significant contrast indicating no specificity of the ROI in MB. MB: mind-blanking, SDep: stimulus-dependent thoughts, SInd: stimulus-independent thoughts, Sens: perceptions.

systematically deactivated, while the rest varied around 0. These results were consistent across the choices of different priors. No other ROI showed specificity for MB. To further validate whether the fitted models performed better against null models with only one intercept, for each fitted ROI we estimated the Watanabe–Akaike information criterion (WAIC) of the fitted and null model, as well as the expected log pointwise predictive density using leave-one-out cross-validation. Only for betas in the vmPFC/subACC did the model containing multiple intercepts perform better than the null model ($\text{Fitted}_{\text{WAIC}}$ −129.687 < $\text{Null}_{\text{WAIC}}$: −129.833, $\text{Fitted}_{\text{ELPD}}$: −129.868 < $\text{Null}_{\text{ELPD}}$: −129.908; Table 3). The validity of the model fit, as well as the specificity of the vmPFC/ACC cluster in MB was replicated across all examined prior distributions for every model.

Discussion

We re-analyzed an fMRI experience-sampling dataset to study the neural correlates of mind-blanking (MB) during unconstrained thinking and explore how instructions affect these correlates. Compared with mental states with reportable content, our findings indicate that spontaneous MB is linked to widespread deactivations in thalamo-cortical networks, which deviate from previous results.

Widespread thalamo-cortical deactivations are linked to MB reports

We first show that whole-brain, thalamo-cortical deactivations precede MB reports. The fMRI univariate analysis, examining positive and negative effects of MB, yielded deactivations in the anterior cingulate and calcarine cortex, the bilateral thalami, the

Table 3. Model comparison of fitted models

Region of interest	Model	WAIC	ELPD
vmPFC-ACC	Fitted	−129.687	−129.868
	Null	−129.833	−129.908
Broca's area	Fitted	−93.934	−93.972
	Null	−91.857	−91.877
Left hippocampus	Fitted	−32.831	−32.856
	Null	−30.82	−30.847

WAIC = Watanabe–Akaike information criterion; ELPD = expected log pointwise predictive density.

right anterior insula, the precentral gyrus and the left parietal lobule. Such cortical deactivations have been previously associated with reduced neuronal resource allocation (Hester et al., 2004), task demands (Hairston et al., 2008), and impaired cognitive performance (Ji et al., 2010). Overall, we consider that the identified whole-brain deactivations might represent brief periods of neuronal disengagement, during which the brain cannot support attentional and mental-reporting processes.

This is further supported by the finding that two key subclusters were further deactivated: the primary visual cortex and multiple cortical nodes of the salience network (Seeley et al., 2007). In previous work, thoughts unrelated to the immediate environment correlated with the decoupling of sensory areas from regions contributing to stimulus salience (Mittner et al., 2016). Indeed, instructing participants to think of nothing results in decreased connectivity between the DMN and the sensory cortices, potentially reflecting this decoupling of the sensory system and a system of internal thoughts (Kawagoe et al., 2018). The whole-brain disengagement explanation is also supported by the deactivation of the thalamus, a recurrent node in saliency and engagement in mental state reportability (Kucyi et al., 2013). Thalamic activity covaries with executive control and attentional demands (Jansma et al., 2000; Antonucci et al., 2021). Potentially, the integrative nature of the thalamus (Hwang et al., 2017) is necessary to cast a mental spotlight and selectively allocate resources to bring a specific thought into conscious awareness. Overall, the rich profile of deactivations preceding MB reports highlights the important role of cortical nodes, traditionally associated with the salience of information.

On our quest to better understand the neuronal significance of such deactivations, we could resort to recent findings that analyzed the same dataset but examined functional connectivity. In that work, we show that MB reports are associated with a hypersynchronized fMRI cortical connectivity profile, further characterized by high global signal amplitude, which we interpreted as neuronal down-states (Mortaheb et al., 2022). Although it would be tempting to hypothesize a similarly low neural activation mediating the identified deactivations, we recognize that a one-to-one comparison between the two analyses is difficult to make, as different aspects of the BOLD signal are examined. Indeed, while task-based BOLD activations can be considered as proxies of neuronal firing (Logothetis et al., 2001), changes in resting-state activity can result from complex interactions among neural, vascular, and metabolic factors (Liu, 2013). As a result, it is not clear whether there is a direct mapping between BOLD activations and functional connectivity analyses.

MB-specific deactivations are linked to parietal and frontal regions

Moving to report-specific effects by contrasting presence versus absence of content we also found that MB is characterized by deactivations in the left angular gyrus. Supporting variant mnemonic (Ciaramelli et al., 2008), attentional (Cattaneo et al., 2009), and semantic processes (Kuhnke et al., 2023), the angular gyrus is recurrently present in content-oriented mental states. Indeed, angular activations have been correlated with both mind-wandering during ongoing mentation (Christoff et al., 2004; Maillet et al., 2019) and external orientation of thought during task engagement across demanding and nondemanding tasks (Turnbull et al., 2019). Therefore, the idea of generalized contributions of the angular gyrus to content-oriented mental states is further supported by our finding of inability to report mental content during deactivation of this region. Our results also are in line with previous electrophysiological results, where MB attentional lapses during task were predicted by posterior EEG slow-wave activity (Andrillon et al., 2021). The authors emphasized the role of parietal cortices in the emergence of conscious reports, where slow-wave activity might inhibit parietal-frontal communication and lead to the MB experience. We supplement this explanation by proving more granular structural information, introducing the angular gyrus as an important parietal node.

By performing an ROI analysis to examine previously reported MB-specific cortical areas, we found MB deactivations in the ACC/vmPFC. In the context of thought-content, frontal activations were observed during mind-wandering with no meta-awareness compared with periods of mind-wandering with meta-awareness. The authors interpreted these larger activations as the ACC signaling a mismatch between expected thought stream and actual, wandering thoughts, eliciting a higher degree of surprise to the participant (Christoff et al., 2009). Additionally, vmPFC activation is correlated with episodic and social self-generated thought (Konu et al., 2020). However, given the multiple partitions of the ACC, treating it as a unimodal region that collectively contributes to one specific cognitive process might be misleading. In our study, the cluster originated close to the borders between ACC and vmPFC, denoting that the previous activation might include multiple processes (a detailed account can be found in https://neurosynth.org/locations/?x=4&%20y=40&z=-4). Indeed, the vmPFC-ACC cluster is systematically implicated in evaluative (D'Argembeau, 2013) and metacognitive processes (Vaccaro and Fleming, 2018), which are facilitatory to the internal stream of thought (Smallwood et al., 2012). Given the self-evaluative aspect of ACC-vmPFC, we here interpret these deactivations as failures to recurrently examine the content of a thought, which can be formulated as self-referential questions ("Am I thinking of anything?"; D'Argembeau et al., 2007).

MB as the mental state of "no thought"

A series of studies has explored ongoing thought using multidimensional experience sampling questionnaires, aiming to decompose it into a low-dimensional space where all content types can be represented (Konu et al., 2020, 2021; Mulholland et al., 2022). Interestingly, this approach has revealed an overlap in the low-dimensional space of ongoing thought-content between everyday life and in-lab task engagement, with consistent clusters related to social cognition, intrusive unpleasant thoughts, and task focus (Konu et al., 2021; Mulholland et al., 2022). In this space, where each dimension represents different content, we suggest that MB could represent the origin point, devoid of specific thought engagement, while moving away from this point would result in clearer content. Conversely, thoughts closer to the origin would exhibit less clearly reportable content.

The activation patterns observed in the ventromedial prefrontal cortex (vmPFC) for thoughts along the social-episodic axis (Konu et al., 2020) and in the parietal lobule for thoughts along the task-focus axis (Turnbull et al., 2019) support this idea, as both these regions are deactivated during MB reports.

Intentional and unintenional MB

So far, only one study has examined the fMRI neural correlates of MB from a univariate perspective (Kawagoe et al., 2019). In that protocol, participants were instructed to "think of nothing" resulting in deactivations in Broca's area and the left hippocampus, and activations in ACC. Similar frontal activations have been observed in clinical settings, where patients with depressive symptoms were guided to suppress their thoughts (Carew et al., 2015). By bridging the current literature together, we suggest that the discrepancy between uninduced and self-induced MB may reflect the existence of different forms of MB, similar to mind-wandering, for which intentional and unintentional forms have been proposed (Seli et al., 2016). Intentional MB may originate from top-down monitoring to exclude thoughts, such as during meditation, while unintentional MB may arise from spontaneous lapses in frontal-parietal-sensory-thalamic systems that monitor the stream of consciousness and guide the ability to attribute semantic content to mental life. While this interpretation is still speculative and the clear presence of different MB forms cannot be extrapolated from our dataset, it paves a promising avenue for future research contrasting different forms of "thought absence".

Limitations and conclusions

Several limitations pertain our study. The duration and sampling rate of mental states, including MB, in fMRI experience-sampling studies may lead to under-sampling of infrequent and transient states (Mortaheb et al., 2022). Complementary methods, such as EEG, which allow for subsecond level estimation of brain dynamics, could provide valuable insights into momentary markers of MB. Additionally, the standard GLM-summary statistics approach may be suboptimal because of the fundamental unbalanced count of different mental states, resulting in reduced statistical power. In that sense, although the here identified effects remain safeguarded, we might nevertheless have missed others because of underpowered statistics. Finally, multivariable decoding approaches varying the duration of mental states could overcome the assumption of uniformity of mental state duration.

In conclusion, we investigated the neural correlates of uninduced MB during free-thinking conditions and found wide-spread thalamo-cortical deactivations, which may not allow the formulation of an efficient neural substrate to serve content reporting. We think that these results provide mechanistic insights on the phenomenology of MB and point to the possibility of MB being expressed in different forms. As MB holds experimental, philosophical, and potential clinical implications for understanding the thought-oriented and stimulus-driven mind, we believe future research would benefit by incorporating MB in the investigation of unconstrained thinking.

References

Andrillon T, Windt J, Silk T, Drummond SPA, Bellgrove MA, Tsuchiya N (2019) Does the mind wander when the brain takes a break? Local sleep in wakefulness, attentional lapses and mind-wandering. Front Neurosci 13:949.

Andrillon T, Burns A, Mackay T, Windt J, Tsuchiya N (2021) Predicting lapses of attention with sleep-like slow waves. Nat Commun 12:3657.

Antonucci LA, Penzel N, Pigoni A, Dominke C, Kambeitz J, Pergola G (2021) Flexible and specific contributions of thalamic subdivisions to human cognition. Neurosci Biobehav Rev 124:35–53.

Boulakis PA (2023) Replication codes for "Whole-Brain Deactivations Precede Uninduced Mind-Blanking Reports".GitLab 10.5281/zenodo.8302116.

Carew CL, Tatham EL, Milne AM, MacQueen GM, Hall GB (2015) Design and implementation of an fMRI study examining thought suppression in young women with, and at-risk, for depression. J Vis Exp (99):e52061.

Cattaneo Z, Silvanto J, Pascual-Leone A, Battelli L (2009) The role of the angular gyrus in the modulation of visuospatial attention by the mental number line. Neuroimage 44:563–568.

Christoff K, Ream JM, Gabrieli JDE (2004) Neural basis of spontaneous thought processes. Cortex 40:623–630.

Christoff K, Gordon AM, Smallwood J, Smith R, Schooler JW (2009) Experience sampling during fMRI reveals default network and executive system contributions to mind wandering. Proc Natl Acad Sci U S A 106:8719–8724.

Ciaramelli E, Grady CL, Moscovitch M (2008) Top-down and bottom-up attention to memory: a hypothesis (AtoM) on the role of the posterior parietal cortex in memory retrieval. Neuropsychologia 46:1828–1851.

Crespo-García M, Wang Y, Jiang M, Anderson MC, Lei X (2022) Anterior cingulate cortex signals the need to control intrusive thoughts during motivated forgetting. J Neurosci 42:4342–4359.

D'Argembeau A (2013) On the role of the ventromedial prefrontal cortex in self-processing: the valuation hypothesis. Front Hum Neurosci 7:372.

D'Argembeau A, Ruby P, Collette F, Degueldre C, Balteau E, Luxen A, Maquet P, Salmon E (2007) Distinct regions of the medial prefrontal cortex are associated with self-referential processing and perspective taking. J Cogn Neurosci 19:935–944.

Demertzi A, Soddu A, Laureys S (2013) Consciousness supporting networks. Curr Opin Neurobiol 23:239–244.

El-Baba M, Lewis DJ, Fang Z, Owen AM, Fogel SM, Morton JB (2019) Functional connectivity dynamics slow with descent from wakefulness to sleep. PLoS One 14:e0224669.

Hairston WD, Hodges DA, Casanova R, Hayasaka S, Kraft R, Maldjian JA, Burdette JH (2008) Closing the mind's eye: deactivation of visual cortex related to auditory task difficulty. Neuroreport 19:151–154.

Harrison RL (2010) Introduction to Monte Carlo simulation. AIP Conf Proc 1204:17–21.

Hester RL, Murphy K, Foxe JJ, Foxe DM, Javitt DC, Garavan H (2004) Predicting success: patterns of cortical activation and deactivation prior to response inhibition. J Cogn Neurosci 16:776–785.

Hoffman MD, Gelman A (2014) The No-U-turn sampler: Adaptively setting path lengths in Hamiltonian Monte Carlo. J Mach Learn Res 15:1593–1623.

Hwang K, Bertolero MA, Liu WB, D'Esposito M (2017) The human thalamus is an integrative hub for functional brain networks. J Neurosci 37:5594–5607.

Jansma JM, Ramsey NF, Coppola R, Kahn RS (2000) Specific versus nonspecific brain activity in a parametric N-back task. Neuroimage 12:688–697.

Jenkins AC, Mitchell JP (2011) Medial prefrontal cortex subserves diverse forms of self-reflection. Soc Neurosci 6:211–218.

Ji G, Sun H, Fu Y, Li Z, Pais-Vieira M, Galhardo V, Neugebauer V (2010) Cognitive impairment in pain through amygdala-driven prefrontal cortical deactivation. J Neurosci 30:5451–5464.

Kawagoe T, Onoda K, Yamaguchi S (2018) Different pre-scanning instructions induce distinct psychological and resting brain states during functional magnetic resonance imaging. Eur J Neurosci 47:77–82.

Kawagoe T, Onoda K, Yamaguchi S (2019) The neural correlates of "mind blanking": when the mind goes away. Hum Brain Mapp 40:4934–4940.

Konu D, Turnbull A, Karapanagiotidis T, Wang HT, Brown LR, Jefferies E, Smallwood J (2020) A role for the ventromedial prefrontal cortex in self-generated episodic social cognition. Neuroimage 218:116977.

Konu D, Mckeown B, Turnbull A, Siu Ping Ho N, Karapanagiotidis T, Vanderwal T, McCall C, Tipper SP, Jefferies E, Smallwood J (2021) Exploring patterns of ongoing thought under naturalistic and conventional task-based conditions. Conscious Cogn 93:103139.

Kucyi A, Salomons TV, Davis KD (2013) Mind wandering away from pain dynamically engages antinociceptive and default mode brain networks. Proc Natl Acad Sci U S A 110:18692–18697.

Kuhnke P, Chapman CA, Cheung VKM, Turker S, Graessner A, Martin S, Williams KA, Hartwigsen G (2023) The role of the angular gyrus in semantic cognition: a synthesis of five functional neuroimaging studies. Brain Struct Funct 228:273–291.

Liu TT (2013) Neurovascular factors in resting-state functional MRI. Neuroimage 80:339–348.

Logothetis NK, Pauls J, Augath M, Trinath T, Oeltermann A (2001) Neurophysiological investigation of the basis of the fMRI signal. Nature 412:150–157.

Maillet D, Beaty RE, Adnan A, Fox KCR, Turner GR, Spreng RN (2019) Aging and the wandering brain: age-related differences in the neural correlates of stimulus-independent thoughts. PLoS One 14:e0223981.

McElreath R (2020) Statistical rethinking: a Bayesian course with examples in R and STAN, Ed 2. New York: Chapman and Hall/CRC.

Mittner M, Hawkins GE, Boekel W, Forstmann BU (2016) A neural model of mind wandering. Trends Cogn Sci 20:570–578.

Mortaheb S, Van Calster L, Raimondo F, Klados MA, Boulakis PA, Georgoula K, Majerus S, Van De Ville D, Demertzi A (2022) Mind blanking is a distinct mental state linked to a recurrent brain profile of globally positive connectivity during ongoing mentation. Proc Natl Acad Sci U S A 119:e2200511119.

Mulholland B, Goodall-Halliwell I, Wallace R, Chitiz L, Mckeown B, Rastan A, Poerio G, Leech R, Turnbull A, Klein A, Auken W, Milham M, Wammes J, Jefferies E, Smallwood J (2022) Patterns of ongoing thought in the real-world. Conscious Cogn 114:103530.

Power JD, Barnes KA, Snyder AZ, Schlaggar BL, Petersen SE (2012) Spurious but systematic correlations in functional connectivity MRI networks arise from subject motion. Neuroimage 59:2142–2154.

Qin P, Wang M, Northoff G (2020) Linking bodily, environmental and mental states in the self—a three-level model based on a meta-analysis. Neurosci Biobehav Rev 115:77–95.

Salvatier J, Wiecki TV, Fonnesbeck C (2016) Probabilistic programming in Python using PyMC3. PeerJ Comput. Sci 2:e55.

Seeley WW, Menon V, Schatzberg AF, Keller J, Glover GH, Kenna H, Reiss AL, Greicius MD (2007) Dissociable intrinsic connectivity networks for salience processing and executive control. J Neurosci 27:2349–2356.

Seli P, Risko EF, Smilek D, Schacter DL (2016) Mind-wandering with and without intention. Trends Cogn Sci 20:605–617.

Smallwood J, Schooler JW (2015) The science of mind wandering: empirically navigating the stream of consciousness. Annu Rev Psychol 66:487–518.

Smallwood J, Brown K, Baird B, Schooler JW (2012) Cooperation between the default mode network and the frontal-parietal network in the production of an internal train of thought. Brain Res 1428:60–70.

Smallwood J, Turnbull A, Wang HT, Ho NSP, Poerio GL, Karapanagiotidis T, Konu D, Mckeown B, Zhang M, Murphy C, Vatansever D, Bzdok D, Konishi M, Leech R, Seli P, Schooler JW, Bernhardt B, Margulies DS, Jefferies E (2021) The neural correlates of ongoing conscious thought. iScience 24:102132.

Taylor PA, Reynolds RC, Calhoun V, Gonzalez-Castillo J, Handwerker DA, Bandettini PA, Mejia AF, Chen G (2023) Highlight results, don't hide them: enhance interpretation, reduce biases and improve reproducibility. Neuroimage 274:120138.

Turnbull A, Wang HT, Murphy C, Ho NSP, Wang X, Sormaz M, Karapanagiotidis T, Leech RM, Bernhardt B, Margulies DS, Vatansever D, Jefferies E, Smallwood J (2019) Left dorsolateral prefrontal cortex supports context-dependent prioritisation of off-task thought. Nat Commun 10:3816.

Vaccaro AG, Fleming SM (2018) Thinking about thinking: a coordinate-based meta-analysis of neuroimaging studies of metacognitive judgements. Brain Neurosci Adv 2:2398212818810591.

Van Calster L, D'Argembeau A, Salmon E, Peters F, Majerus S (2017) Fluctuations of attentional networks and default mode network during the resting state reflect variations in cognitive states: evidence from a novel resting-state experience sampling method. J Cogn Neurosci 29:95–113.

Vanhaudenhuyse A, Demertzi A, Schabus M, Noirhomme Q, Bredart S, Boly M, Phillips C, Soddu A, Luxen A, Moonen G, Laureys S (2011) Two distinct neuronal networks mediate the awareness of environment and of self. J Cogn Neurosci 23:570–578.

Ward A, Wegner D (2013) Mind-blanking: when the mind goes away. Front Psychol 4:650.

Weinstein Y (2018) Mind-wandering, how do I measure thee with probes? Let me count the ways. Behav Res Methods 50:642–661.

Winter U, LeVan P, Borghardt TL, Akin B, Wittmann M, Leyens Y, Schmidt S (2020) Content-free awareness: EEG-fcMRI correlates of consciousness as such in an expert meditator. Front Psychol 10:3064.